



OPEN

# Injectable bone cement based on magnesium potassium phosphate and cross-linked alginate hydrogel designed for minimally invasive orthopedic procedures

Marcin Wekwejt<sup>1✉</sup>, Rafał Jesiołkiewicz<sup>2</sup>, Aleksandra Mielewczyk-Gryń<sup>3</sup>, Dawid Kozień<sup>4</sup>, Anna Ronowska<sup>5</sup>, Justyna Kozłowska<sup>6</sup> & Uwe Gbureck<sup>7</sup>

Bone cement based on magnesium phosphate has extremely favorable properties for its application as a bioactive bone substitute. However, further improvement is still expected due to difficult injectability and high brittleness. This paper reported the preparation of novel biocomposite cement, classified as dual-setting, obtained through ceramic hydration reaction and polymer cross-linking. Cement was composed of magnesium potassium phosphate and sodium alginate cross-linked with calcium carbonate and gluconolactone. The properties of the obtained composite material and the influence of sodium alginate modification on cement reaction were investigated. Our results indicated that proposed cements have several advantages compared to ceramic cement, like shortened curing time, diverse microstructure, increased wettability and biodegradability and improved paste cohesion and injectability. The magnesium phosphate cement with 1.50% sodium alginate obtained using a powder-to-liquid ratio of 2.5 g/mL and cross-linking ratio 90/120 of GDL/CC showed the most favorable properties, with no adverse effect on mechanical strength and osteoblasts cytocompatibility. Overall, our research suggested that this novel cement might have promising medical application prospects, especially in minimally invasive procedures.

**Keywords** Bone cement, Magnesium potassium phosphate, Sodium alginate, Biocomposite, Dual-setting cement

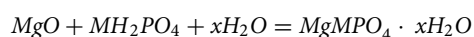
## Abbreviations

|       |   |
|-------|---|
| ANOVA | Analysis of variance                    |
| BC    | Bone cement                             |
| CC    | Calcium carbonate                       |
| CaP   | Calcium phosphate                       |
| CS    | Compression strength                    |
| GDL   | Glucono-delta-lactone                   |
| FTIR  | Fourier-transform infrared spectroscopy |
| hFOB  | Human osteoblast cell line              |

<sup>1</sup>Biomaterials Technology Department, Faculty of Mechanical Engineering and Ship Technology, Gdańsk University of Technology, Gdańsk, Poland. <sup>2</sup>Scientific Club 'Materials in Medicine', Advanced Materials Centre, Gdańsk University of Technology, Gdańsk, Poland. <sup>3</sup>Department of Ceramic, Faculty of Applied Physics and Mathematics, Gdańsk University of Technology, Gdańsk, Poland. <sup>4</sup>Faculty of Materials Science and Ceramics, AGH University of Kraków, Kraków 30-059, Poland. <sup>5</sup>Chair of Clinical Biochemistry, Department of Laboratory Medicine, Medical University of Gdańsk, Gdańsk, Poland. <sup>6</sup>Department of Biomaterials and Cosmetics Chemistry, Nicolaus Copernicus University in Toruń, Toruń, Poland. <sup>7</sup>Department for Functional Materials in Medicine and Dentistry, University of Würzburg, Würzburg, Germany. ✉email: marcin.wekwejt@pg.edu.pl

|      |   |
|------|---|
| ICDD | International centre for diffraction data |
| Mg/P | Magnesium-to-phosphate                    |
| MPC  | Magnesium phosphate cement                |
| MTT  | Thiazolyl blue tetrazolium tromide        |
| PBS  | Phosphate-buffered saline                 |
| PMMA | Poly(methyl methacrylate)                 |
| P/L  | Powder-to-liquid                          |
| SA   | Sodium alginate                           |
| SEM  | Scanning electron microscopy              |
| SD   | Standard deviations                       |
| TCP  | Tissue culture plate                      |
| XRD  | X-ray diffractometer                      |
| YM   | Young Modulus                             |

Bone, like other tissues in the human body, has the ability to regenerate. However, in the case of complex problems such as defects, injuries or diseases, e.g. osteoporosis, the bone tissue will not heal on its own and external intervention is necessary<sup>1</sup>. Various injectable synthetic bone substitutes, based on biopolymers or bioceramics, are currently proposed for medical applications. A fascinating group of biomaterials is also self-hardening bone cement, which can be used to stabilize complex fractures or fill bone defects<sup>2,3</sup>. The leading group of ceramic cement is calcium phosphates, which are similar in composition to bone<sup>3</sup>. On the other hand, magnesium phosphates (MPC) are less popular on the medical market but also an exciting alternative. Despite being less common in biomedical applications, MPC offers unique advantages: it sets and hardens faster than CPC, thereby facilitating easier application, provides immediate structural support, degrades more quickly and finally leads to accelerated recovery<sup>4</sup>. Further, MPC demonstrates superior mechanical strength and osteogenic potential, which may be particularly advantageous in scenarios of osteoporotic bones or meeting the requirements for bonding surrounding tissues<sup>5,6</sup>. This ceramic cement is set by an acid-base reaction of magnesia (MgO) with various water-soluble phosphates, for example, according to the reaction below<sup>7</sup>:



where M = Na, NH<sub>4</sub> or K.

MPC is characterized by more effective resorption in the body, better initial mechanical properties and shortened setting time<sup>8,9</sup>. Moreover, Mg ions released from MPC have osteogenic and antibacterial properties<sup>10</sup>. In recent years, intensive research has been underway to optimize this cement production, focusing i.e. on various compositions, different powder-to-liquid ratios and/or novel technologies<sup>9,11</sup>. Another approach that also seems reasonable is the development of innovative composite cements based on MPC with various polymer additives. Such research was carried out previously, for example, by Zárbybnická et al. (MPC + polyvinyl alcohol; MPC + latex)<sup>12,13</sup>, Gong et al. (oxygen-carboxymethyl chitosan)<sup>14</sup> or Tang et al. (polyethylene fibers)<sup>15</sup>. The cements obtained in those studies exhibited significantly improved properties, including setting reaction, biodegradation, and mechanical strength. On the other hand, here, we proposed a novel composite bone cement based on MPC enriched with cross-linked alginate hydrogel.

Hydrogels belong to a three-dimensional group of soft materials created through cross-linking processes. They are characterized by high hydrophilicity and specific physiological functions depending on their application. Additionally, they are used in various fields such as medicine, biotechnology, pharmacy, cosmetology, and materials engineering<sup>16</sup>. In this work, sodium alginate (SA) was chosen as the hydrogel phase. SA is a biopolymer of natural origin that may be found in the brown algae walls (*Phaeophyceae*) or bacterial organisms such as *Azotobacter* and *Pseudomonas*. Its presence generally contributes to increased flexibility while maintaining the appropriate and stable structure of the algae. This is very important in protecting these plants from potential damage during intense waves occurring in storms<sup>17</sup>. AS showed favorable properties, including high biocompatibility, effective gelation and degradability, gaining broader application in the various industry markets. For example, it is used as an emulsifier and stabilizer in the food industry<sup>18</sup>, a drug carrier or matrix for delivering different proteins or cells<sup>19</sup>, wound dressing material<sup>20</sup>, and also as the biological substitute for soft tissue in bioengineering<sup>21</sup>. Recently, sodium alginate was also considered by Liu et al. as a retarder of the hydration reaction of MPC cement<sup>22</sup>. They found that SA (up to 2%) delayed the dissolution of potassium dihydrogen phosphate similar to boric acid. Here, MPC was modified with alginate hydrogel cross-linking by the delayed reaction of gluconolactone and calcium carbonate, previously described in the literature<sup>23</sup>. Moreover, the cement we developed belongs to the highly fascinating group of so-called dual-setting bone cements<sup>24</sup>.

In this study, the effect of alginate hydrogel as an additive to magnesium phosphate cement was tested. Sodium alginate solutions were used as the aqueous phase of cement, instead of distilled water. The hydrogel was cross-linked in a delayed reaction of calcium carbonate controlled by gluconolactone<sup>25</sup>. This research aimed to evaluate the impact of the proposed modification on functional, mechanical and biological cement properties. As a result of the conducted research, we developed a technology for obtaining a novel dual-setting composite bone cement that may be used in minimally orthopedic invasive surgery.

## Materials and methods

### Cement preparation

In this study, a powder phase of MPC was made from dead burn magnesia powder (calcined under 1500 °C / 5 h; ~ 9.04 ± 0.44 μm; Fisher Chemical, USA), and potassium dihydrogen phosphate (KH<sub>2</sub>PO<sub>4</sub>, ~ 78.1 ± 0.44 μm, Chempur, PL) mixed in a 4:1 molar ratio. While aqueous solutions of sodium alginate (SA; Chemat, PL) were

used as a liquid phase.  $\delta$ -Gluconolactone (GDL; ThermoScientific, USA – added to powder component of cement) and calcium carbonate (CC; Chempur, PL – added to the liquid component of cement) were used to cross-link the hydrogel. At the preliminary research stage, variable technological parameters were selected, such as 1.25% or 1.5% SA w/v concentration, 2.0 or 2.5 powder-to-liquid ratio and 90/120 or 120/150 GDL/CC ratio. The GDL/CC ratio was selected based on previous research<sup>25</sup>. Mix proportions applied in the experiments are listed in Table 1 (and also in weight form in Table S1). The cement specimens were prepared by mixing the powder component (MgO, KH<sub>2</sub>PO<sub>4</sub> + GDL) with a liquid component (SA + CC) in a plastic bowl and manually stirring until obtaining a homogeneous paste. Next, the paste was transferred into silicone rubber molds (in two forms: cubic: 6 × 6 × 12 mm and disk: 2 × 15 mm) and stored for curing for a minimum of 24 h in a water bath (~ 36.6 °C and > 90% humidity; Chemland, Poland). The average particle size of powders was determined using the SALD-2300 particle size analyzer (Shimadzu, Japan).

Unmodified MPC cement with Mg/P 4:1 and P/L 2.5 P/L ratios and, in some research, MPC cement containing sodium alginate (MPC + SA) as well without additional cross-linking were selected as controls in our study. The sample photo of tested bone cements after curing for 24 h is shown in Fig. S1.

## Characterization

### Setting time and setting temperature

The setting time of cement paste ( $n = 3$ ) was measured using the Vicat MMC-045/E apparatus (Multiserw-Morek, Poland) with a metallic needle (diameter 1.13 mm) and a load of 300 g. This time was considered from the cement components combination to when specimens were fully solidified, and the indentation mark was not visible on their surface. While the setting temperature of cement ( $n = 3$ ) was tested using a thermocouple (Czah, Poland) and the maximum value was recorded. For this experiment, cement paste obtained from one gram of cement powder was put in a 2 mL eppendorf into which the meter was inserted.

### Microstructure analysis

After their curing and drying, the surface microstructure of the obtained cement was examined by high-resolution Scanning Electron Microscope (SEM) Quanta 250 FEG (FEI, USA). Before an examination, all specimens were stuck on special holders via conductive stickers and were then sputtered with a thin (10 nm) gold layer using a high vacuum EM SCD500 sputtering machine (Leica, Germany) for electron reflection. SEM images were taken for each specimen in three different locations at three magnifications: 500x, 1000x and 2000x. The images were analyzed using the ImageJ program (measurements  $n = 20$ ).

### Phase and chemical groups

The cements, after hardening and curing, were analyzed by attenuated total reflection infrared spectroscopy (ATR-FTIR) with the usage of Nicolet iS5 spectrometer (Thermo Fisher Scientific, Waltham, MA, USA) equipped with an ATR device. The 4000 to 500 cm<sup>-1</sup> spectra were collected at room temperature at a resolution of 4 cm<sup>-1</sup> and with 64 scans. ZnSe was used as an ATR crystal. The spectra were acquired in the transmission mode, normalized and smoothed. Further, specimens were crushed and ground in a mortar and then analyzed by a Phillips Panalytical X'PERT PRO X-ray diffractometer (Almelo, The Netherlands) using Cu-K $\alpha$  radiation. Data were collected from 2 $\theta$  = 5–90° with a step size of 0.02°, a 40 kV voltage and a 40 mA current. The phase identification has been undertaken using HighScore Plus software with the Inorganic Crystal Structure Database (ICSD) database, safety data sheets were used for struvite (ICSD 98-006-0626) and magnesium oxide (ICSD 98-015-7523).

### Surface wettability

The surface wettability was determined on dry cement specimens by water contact angle measurements with an optical tensiometer (Attention Theta Life, Biolin Scientific, Finland) based on the falling drop method (volume ~ 1  $\mu$ L;  $n = 5$ ).

### Porosity

The initial porosity  $\Phi$  (%) of the cements ( $n = 3$ ) was calculated by the following Eq. 1<sup>1</sup>:

$$\Phi = (m_w - m_d) / (\rho \cdot V) \cdot 100\%$$

| Cement name                        | SA    | P/L ratio | GDL/CC ratio |
|------------------------------------|-------|-----------|--------------|
| MPC                                | –     | 2.5       | –            |
| MPC + 1.25%SA                      | 1.25% | 2.5       | –            |
| MPC + 1.50%SA                      | 1.50% | 2.5       | –            |
| MPC + 1.25%SA_2.0P/L_120/150GDL/CC | 1.25% | 2.0       | 120/150      |
| MPC + 1.50%SA_2.0P/L_90/120GDL/CC  | 1.50% | 2.0       | 90/120       |
| MPC + 1.25%SA_2.5P/L_120/150GDL/CC | 1.25% | 2.5       | 120/150      |
| MPC + 1.50%SA_2.5P/L_90/120GDL/CC  | 1.50% | 2.5       | 90/120       |

**Table 1.** Mix proportions of tested composite bone cements.

where  $m_d$  is the dry mass,  $m_w$  is the wet mass (g) after immersion in PBS (when a constant weight is achieved),  $\rho$  is the density of PBS ( $\text{g/cm}^3$ ), and  $V$  is the volume of the specimen ( $\text{cm}^3$ ). The specimens were dried 24 h in the dryer at a temperature of 50 °C.

#### *pH of cement pastes*

The pH changes of cement pastes during the hydration process were evaluated semiquantitatively with universal pH test strips ( $n = 3$ ; Macherey-Nagel, Germany). During the test, the pH values were written every two minutes in the first period of the bone cement setting, up to its hardening. The accuracy of strips was 0.5 pH unit, and every stripe had four indicator fields, which ensured high reading precision.

#### **Mechanical properties**

The static compressive tests ( $n = 5$ ) were performed using a Universal Mechanical Testing Machine Z005 (Zwick, Germany) with a 5 kN load cell and a 1 mm/min crosshead speed. The compressive strength ( $\sigma_c$ ) and compressive modulus ( $E_c$ ) were calculated by a standard method using integrated software testXpert III (Zwick, Germany).

#### **Degradation behavior and in vitro bioactivity**

The dried and hardened cements ( $n = 3$ ) were washed in 1 mL phosphate-buffered saline (PBS) per specimen for 3 h (with a change of solution every hour) to remove possible salt residues in material pores. Then, specimens were dried at 37 °C overnight and weighed (initial mass was determined). Finally, cements were immersed in 2.5 mL of PBS solution (Merck, Germany) and stored for 30 days at 37 °C with a PBS change every third day. After the immersion, specimens were removed from the solution, washed three times using demineralized water, dried overnight and weighed again (final mass was determined). The relative mass loss was calculated by the following Eq. 1<sup>1</sup>:

$$m_{\%} = m_f / m_i \cdot 100\%$$

where  $m_{\%}$  is the mass change (%),  $m_f$  is the final, and  $m_i$  is the initial mass (g). The analytical balance accuracy of the laboratory scale was 1.0 mg. Subsequently, the surfaces of the specimens were analyzed post-immersion in simulated body fluid (SBF) solution utilizing SEM (with a gold layer applied) in conjunction with Energy Dispersive Spectroscopy (EDS; Scios 2DualBeam, ThermoFisher, USA), aimed at evaluating apatite formation.

#### **Cohesion of the paste and injectability**

Injectability was qualitatively assessed by injecting a specified amount of cement paste from a 5 mL syringe into the PBS solution. The cement components were mixed together and transferred to a syringe, then after about 5 min hand squeezed. To illustrate the results, photos were taken after 15 min of performed experiments.

#### **Cytocompatibility**

Cytocompatibility of developed bone cements was evaluated with a human osteoblast cell line (hFOB 1.9; ATCC CRL-11372). Cells were cultured in F12/Dulbecco-Modified Eagle's Medium (Merck, Germany) supplemented with 0.3 mg/mL geneticin sulfate (G-418, ThermoFisher Scientific, UK) and 10% Fetal Bovine Serum (Biowest, France) at 34 °C and 5% CO<sub>2</sub>. Before testing, all specimens ( $n = 4$ ) were sterilized with exposure to UV light ( $2 \times 30$  min) and then immersed in 1.5 mL per specimen in the medium as mentioned earlier for 7 days (pre-treatment) to equalize the ions level<sup>26</sup>. The hFOB cells were seeded at a density of  $80 \times 10^3$  cells/mL on the surface of materials in 1.5 mL of fresh culture medium. The cell viability was analyzed after 3 days of culture using MTT (thiazolyl blue tetrazolium bromide; Merck, Germany) assay. The development of the colored product metabolized by living cells was assessed colorimetrically using a microplate reader (Victor, PerkinElmer, USA) at 595 nm towards reference 690 nm. The results were normalized with a cell incubated on a tissue culture plate-TCP (100%).

#### **Statistics**

Statistical data analysis was performed using commercial software (SigmaPlot 14.0, Systat Software, San Jose, CA, USA). The Shapiro–Wilk test was used to assess the normal distribution of the data. All the results were calculated as means  $\pm$  standard deviations (SD) and statistically analyzed using one-way analysis of variance (one-way ANOVA). Multiple comparisons versus the control group between means were performed using the Bonferroni t-test with the statistical significance set at  $p < 0.05$ .

## **Results**

### **Setting time and temperature**

The addition of alginate hydrogel (with and without cross-linking) contributed to the significant reduction of the setting time in all tested groups of cements (Table 2). However, for groups with 1.25%SA this time was too short than expected for bone cements, as decreased to less than 10 min. In the case of setting temperature (Table 2), adding 1.5% SA did not affect the maximum value, while 1.25% significantly increased it. These differences between SA 1.25% and 1.50% are probably related mostly to the CC/GDL ratio applied for the given group.

### **pH changes during cement setting**

The pH value is important for the proper course of the hydration reaction of MPC, therefore it was also checked whether it was suitable for dual-setting cements. The salt KH<sub>2</sub>PO<sub>4</sub> dissolved in conditions appropriate for

| Cement                             | Setting time (min) | Temperature (°C) |
|------------------------------------|--------------------|------------------|
| MPC                                | 14.55 ± 0.97       | 51.10 ± 0.50     |
| MPC + 1.25%SA                      | 8.27 ± 0.14*       | 53.83 ± 0.55     |
| MPC + 1.50%SA                      | 10.57 ± 0.44*      | 51.03 ± 1.38     |
| MPC + 1.25%SA_2.0P/L_120/150GDL/CC | 8.30 ± 0.30*       | 58.40 ± 2.93*    |
| MPC + 1.50%SA_2.0P/L_90/120GDL/CC  | 13.12 ± 0.88*      | 48.73 ± 0.33     |
| MPC + 1.25%SA_2.5P/L_120/150GDL/CC | 9.26 ± 0.64*       | 58.06 ± 0.27*    |
| MPC + 1.50%SA_2.5P/L_90/120GDL/CC  | 11.58 ± 0.53*      | 49.60 ± 1.06     |

**Table 2.** Setting time and temperature of the tested bone cements ( $n = 3$ , data are expressed as the mean ± SD; \* statistically significant difference as compared to control-MPC ( $p < 0.05$ )).

cement preparation allows to obtain a pH of solution about ~4.5. The addition of GDL (adapting to the GDL/CC ratios: 90 or 120) into this solution changed its pH to 2.0–2.5. Lowering the pH was important to achieve the dissolution of MgO as well as the slow dissolution of CC. The pH changes for the selected cement pastes are shown in Fig. S2 and show the differences in the three stages of the hydration reaction: (1) initial stage (after ~1 min of mixing components), (2) medium stage (about ~4 min) and (3) final stage (about ~8 min). The tested cement showed typical behavior for MPC cement – the initially acidic pH increased over time due to the dissolution of MgO<sup>27</sup>. Further, the dual-setting cements showed an initial reduction of pH (about ~2.0–2.5) due to the addition of SA and GDL.

### Microstructure analysis

The morphology of the hardened cements is shown in Fig. 1, and their crystal size is included in Table S2. In each group, rod-like, randomly oriented crystals of magnesium phosphate were densely packed within a gel-like surface. The pure MPC exhibited crystal with a mean size of ~22 μm. For the groups, MPC + 1.25%SA\_2.5P/L\_120/150GDL/CC and 1.50%SA\_2.0P/L\_90/120GDL/CC, the crystals were slightly smaller, ~12 μm and ~16 μm, respectively. In contrast, the cement MPC + 1.25%SA\_2.0P/L\_120/150GDL/CC exhibited crystal of ~11 μm, while 1.50%SA\_2.5P/L\_90/120GDL/CC of ~16 μm. These crystals grew and formed flower-like structures with sizes ranging from 22 to 85 μm (~57.15 ± 17.83 μm) and 38–92 μm (~64.51 ± 15.19 μm), respectively. It was observed that some of the crystals appeared cracked, likely due to the drying process. Additionally, no visible sodium alginate hydrogel phase was detected in the cement microstructure.

### Phase and chemical composition

The XRD spectra of all tested cements are shown in Fig. 2, and corresponding XRD patterns showed that both pure MPC cement and those modified with sodium alginate hydrogel consisted of a well-crystallized phase of k-struvite-MgKPO<sub>4</sub> × 6H<sub>2</sub>O (ICDD 01-075-1076). No adverse effect of the polymer additive on the MPC hydraulic reactions was confirmed based on no significant changes in XRD patterns. Further, unreacted magnesium oxide – MgO (ICDD 01-075-0447) was also found in each cement, however, it differed in percentage (Table S3).

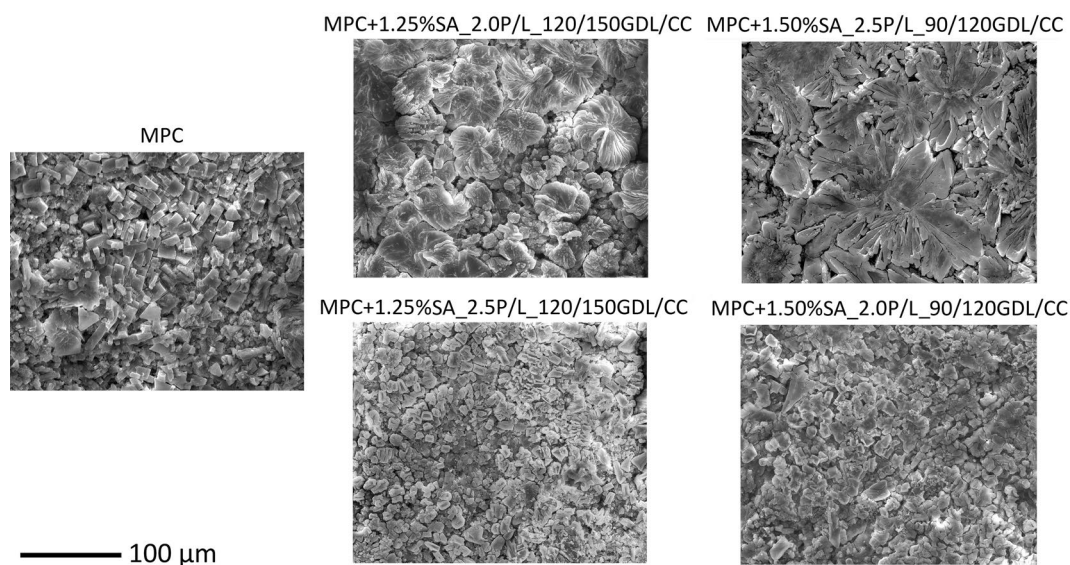


**Fig. 1.** SEM images of the tested bone cements after curing (24 h, 37 °C, 100% humidity) at 500 × magnification after curing (the pictures are representative of three analyses).

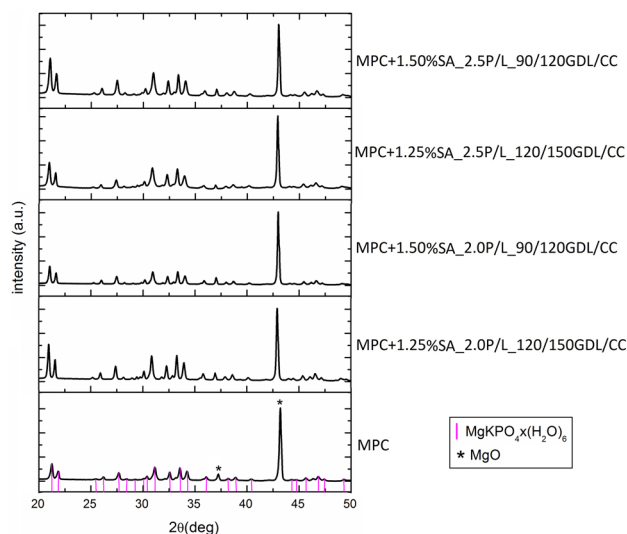


**Fig. 2.** XRD patterns of the tested bone cements after curing (24 h, 37 °C, 100% humidity). Characteristic reflexes are marked as  $\text{MgKPO}_4 \cdot x\text{H}_2\text{O}$  and MgO.

The lowest proportion of magnesium oxide was observed for the groups: MPC + 1.50%SA\_2.5P/L\_90/120GDL/CC (~ 22%) and MPC + 1.25%SA\_2.0P/L\_120/150GDL/CC (~ 38%).

The ATR-IR spectra of all tested cements are shown in Fig. 3, while spectra regarding polymer cross-linking in Fig. S2. In the MPC spectrum, six prominent vibration peaks centered at 2880, 2386, 1588, 988, 693, and 562  $\text{cm}^{-1}$  were observed. The signals in the 3700–1600  $\text{cm}^{-1}$  region were indicated to the O–H,  $\nu(\text{OH})$  and  $\text{H}_2\text{O}$  bendings<sup>28</sup>. The vibration peaks observed at 988, 693 and 562  $\text{cm}^{-1}$  were attributed to the characteristic phosphate groups from k-struvite<sup>22</sup>. Further, according to the current state of knowledge and literature, for sodium alginate spectrum, the O–H stretching vibrations of alginate appeared ~ at 3250  $\text{cm}^{-1}$ , stretching vibrations of C–H at around 2925  $\text{cm}^{-1}$ , COO– stretching at around 1590 and 1410  $\text{cm}^{-1}$ . The peaks at ~ 1295  $\text{cm}^{-1}$  are assigned to the C–O stretching vibration. The band at 1085  $\text{cm}^{-1}$  is related to C–O, C–C, and C–O–C stretching vibrations. The peak at ~ 1030  $\text{cm}^{-1}$  corresponds to the C–C and C–O–C vibrations<sup>28,29</sup>. Moreover, for the spectra of specimens with sodium alginate cross-linked with CC and GDL, three additional peaks were identified at 1736, 1366, and 1217  $\text{cm}^{-1}$ , related to the presence of polymer in the cement and the resulting cross-linking bonds.

### Porosity

Table 3 presents the porosity results of the tested composite MPCs. The addition of hydrogel contributed to a significant decrease in the initial porosity of the cement, except for the MPC + 1.25%SA\_2.0P/L\_120/150GDL/CC group-where it had no significant effect.

### Surface wettability

The graph (Fig. 4) below presents the average wettability angles of each tested hydrogel group and the MPC itself. As can be seen, the influence of the hydrogel resulted in higher angle values, which resulted in a deterioration of the hydrophilicity of the materials. The most hydrophobic material in this study was the MPC + 1.50%SA\_2.5P/L\_90/120GDL/CC group.

### Cohesion and injectability

The control cement (MPC) was injectable, but its cohesion was poor. The use of a hydrogel additive significantly improved both the cohesion of the paste and its ease of injection (Fig. 5). The best improvements in this functional cement parameter were observed for MPC + 1.25%SA\_2.0P/L\_120/150GDL/CC and 1.50%SA\_2.5P/L\_90/120GDL/CC.

### Degradation behavior

The modification significantly affected the biodegradation potential of the specimens as their loss was 1.5–4.0% of their initial mass within a month (Fig. 6). The most significant process was observed for the groups MPC + 1.25%SA\_2.0P/L\_120/150GDL/CC and MPC + 1.50%SA\_2.0P/L\_90/120GDL/CC.

### In vitro bioactivity

After 30 days of incubation in PBS, significant microstructural changes were found in all evaluated cements (Fig. 7). Their surfaces were sparsely covered with spherical particles resembling apatite, primarily consisting of P and Ca (spot 2 on Fig. 7b). However, trace amounts of Mg and K were also identified in the EDS analysis. The precipitates significantly differ in composition from the substrate (k-struvite), in which the presence of Ca

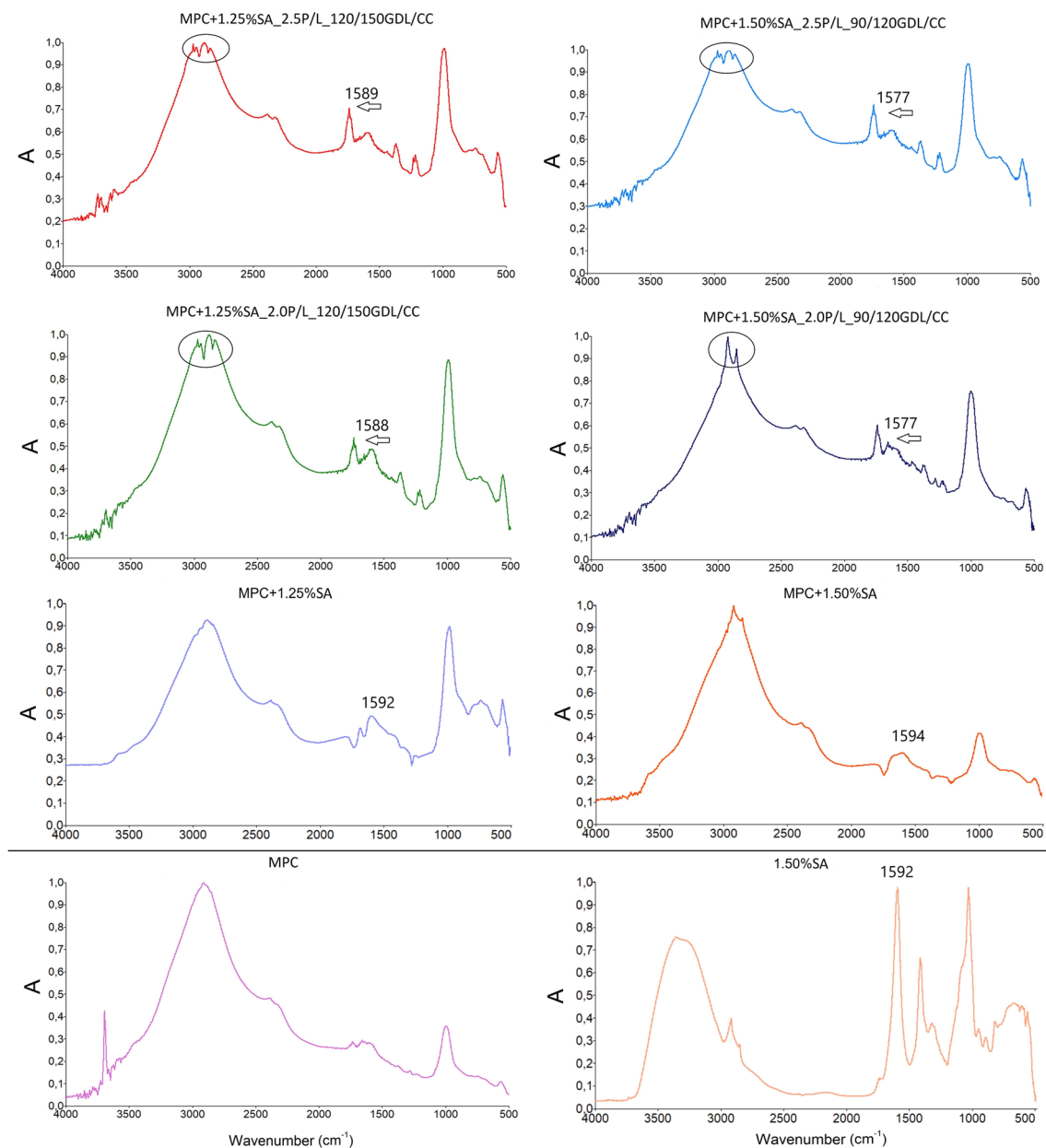


**Fig. 3.** FTIR spectra of the tested bone cements after curing (24 h, 37 °C, 100% humidity; the changes after SA cross-linking in MPC + SA cements were marked).

| Cement                             | Porosity (%) |
|------------------------------------|--------------|
| MPC                                | 7.17 ± 0.46  |
| MPC + 1.25%SA_2.0P/L_120/150GDL/CC | 8.77 ± 1.11  |
| MPC + 1.50%SA_2.0P/L_90/120GDL/CC  | 4.64 ± 0.44* |
| MPC + 1.25%SA_2.5P/L_120/150GDL/CC | 4.08 ± 0.51* |
| MPC + 1.50%SA_2.5P/L_90/120GDL/CC  | 2.64 ± 0.11* |

**Table 3.** Porosity of the tested bone cement ( $n=4$ , data are expressed as the mean ± SD; \* statistically significant difference as compared to control-MPC ( $p < 0.05$ )).

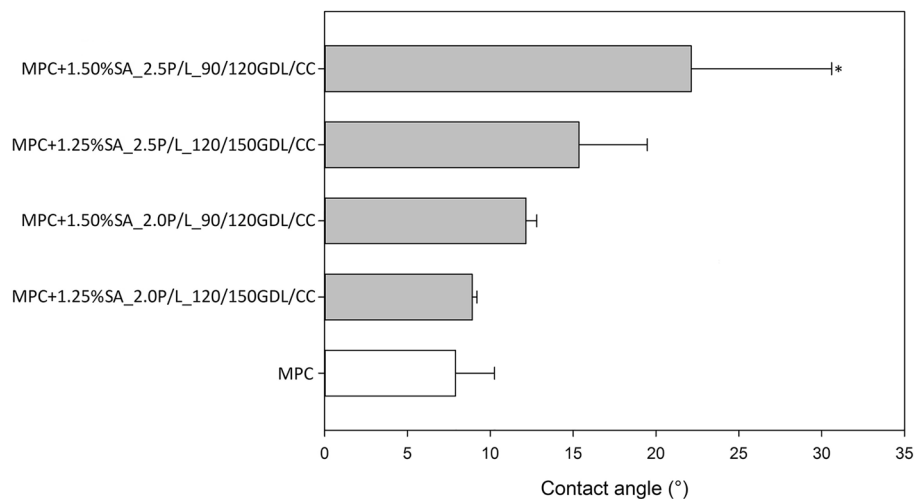


**Fig. 4.** Wettability expressed as the water contact angle for the tested cements after curing ( $n = 5$ , data are expressed as the mean  $\pm$  SD; \* statistically significant difference as compared to control-MPC ( $p < 0.05$ )).

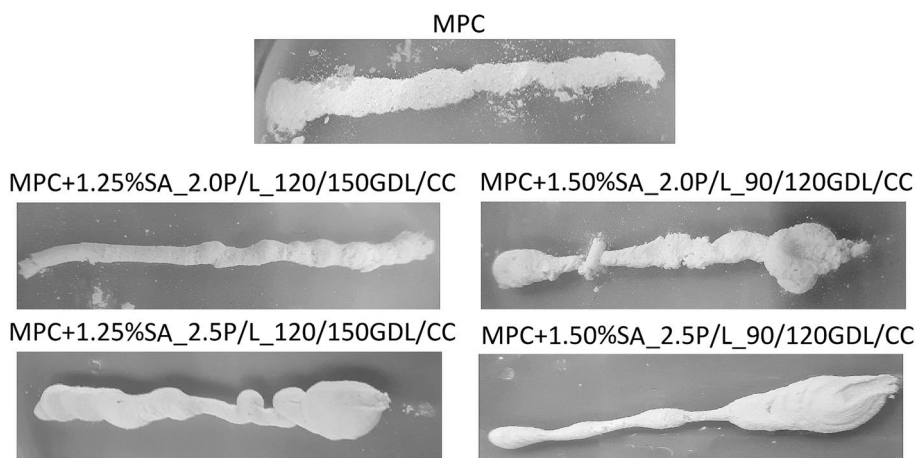


**Fig. 5.** Cohesion and injectability of the tested bone cement pastes (the pictures are representative of three specimens).

was not detected (spot 1 on Fig. 7b). No trend related to the presence of apatite-like particles was observed for the developed cements modified with SA.

### Mechanical properties

The results of compressive strength and compressive modulus are shown in Fig. 8, and mechanical curves are presented in Fig. S3. It was found that the alginate hydrogel negatively affected the mechanical properties of MPC cements. Each tested group showed a significant decrease in compressive strength, except for group MPC + 1.50%SA\_2.0P/L\_90/120GDL/CC. It should, however, be noted that the mean compressive strength value of this group still decreases, but the result does not show a statistically significant difference compared to the MPC cements. Therefore, it can be concluded that the addition of SA has a substantial impact on the mechanical properties of the cement. Further, Young's modulus was decreased for all modified specimens.

### Cytocompatibility

Cytocompatibility studies were performed on human osteoblasts hFOB 1.19, and the results are shown in Fig. 9. Both the pure cement and the modified cements, except MPC + 1.25%SA\_2.0P/L\_120/150GDL/CC showed no cytotoxic effect (cell viability compared to control above 70%). Based on these results, it can be concluded that adding the polymer, in most cases, has no adverse effect on the cytocompatibility of MPC cement. However, the trend of lower cell viability is observable (statistically significant only for 1.25%SA\_2.0P/L\_120/150GDL/CC).



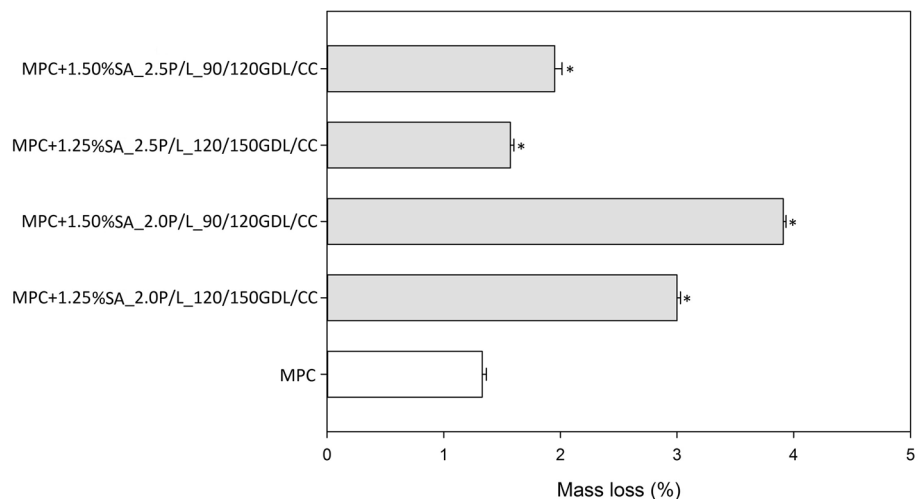


**Fig. 6.** Degradation of the tested cements defined as mass loss after one month of incubation in PBS solution ( $n = 3$ , data are expressed as the mean  $\pm$  SD; \* statistically significant difference as compared to control – MPC ( $p < 0.05$ )).

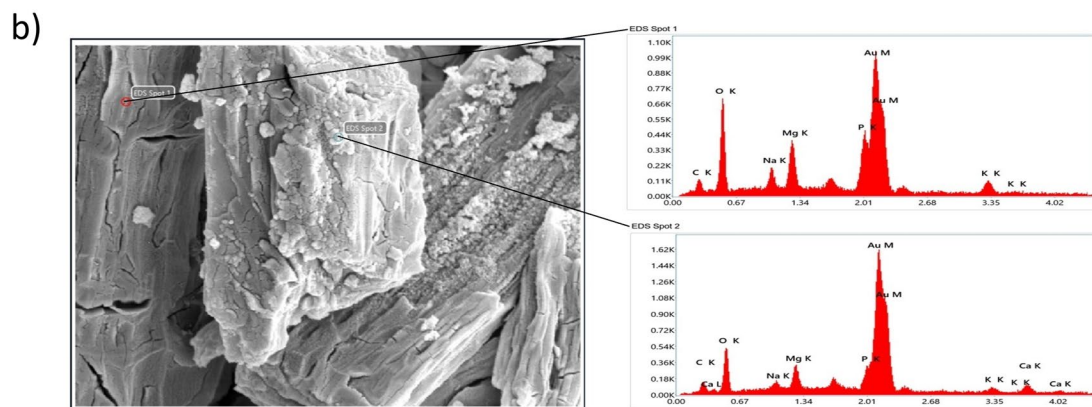
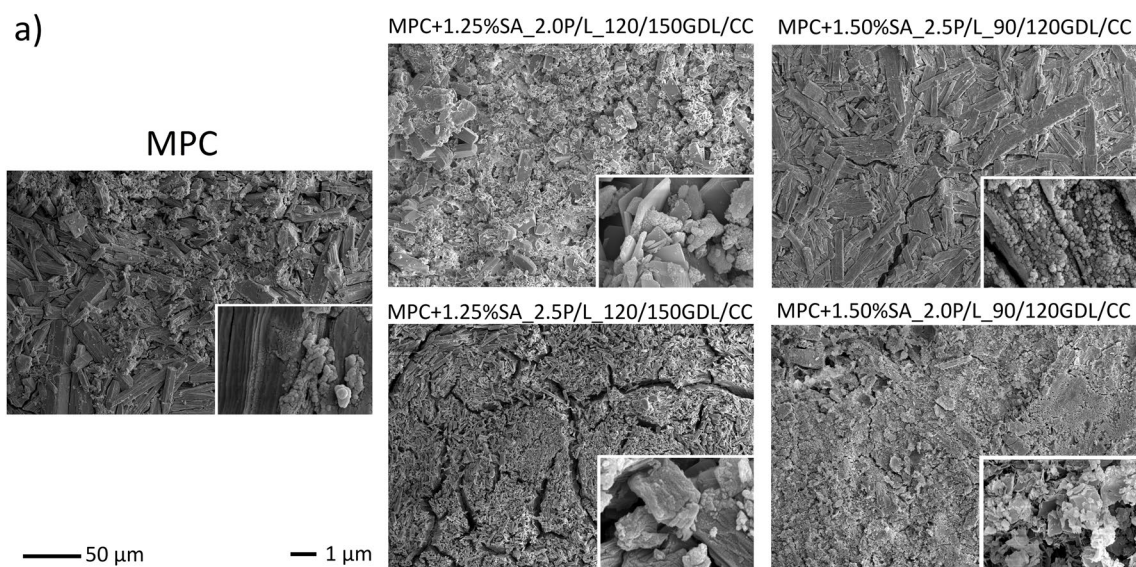


**Fig. 7.** Characterization of the tested cements after one month of incubation in PBS solution: (a) SEM images at 1000 and 50 000 x magnifications and (b) comparative EDS analysis example for different spots.

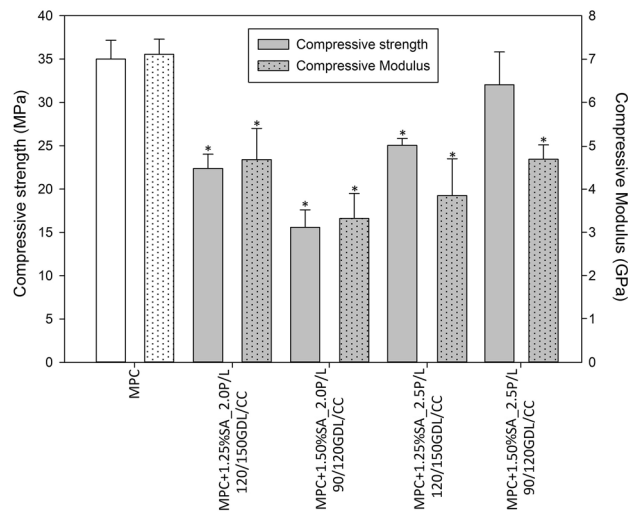


**Fig. 8.** Compression strength ( $\sigma_c$ ) and compressive modulus ( $E_c$ ) of the tested bone cements ( $n=5$ ; data are expressed as the mean  $\pm$  SD; \* statistically significant difference as compared to control-MPC ( $p < 0.05$ )).

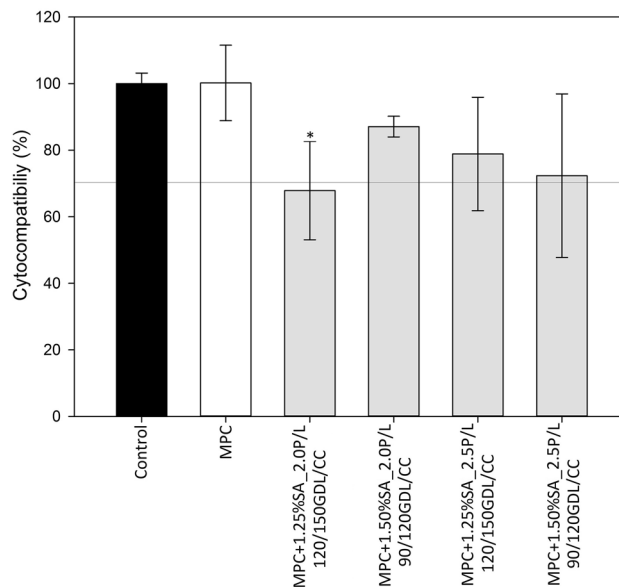


**Fig. 9.** Cytocompatibility results of the tested bone cements on hFOB 1.19 after 3 days of incubation on material surfaces ( $n=4$ ; data are expressed as the mean  $\pm$  SD; line denotes the accepted limit for non-cytotoxic material-ISO 10993-5 standard; \* statistically significant difference as compared to control ( $p < 0.05$ )).

The most optimal for the medical application group may be defined as MPC + 1.50%SA\_2.0P/L\_90/120GDL/CC (MTT:  $\sim 87.1 \pm 3.1\%$ ).

## Discussion

Novel biocomposite bone cements were effectively obtained by optimizing two setting reactions: the hydraulic reaction of dead burn magnesium oxide with potassium dihydrogen phosphate and the cross-linking reaction of the alginate hydrogel, which was confirmed through microstructure analysis and evaluation of chemical and phase composition. Previously, sodium alginate (up to 2%) was proposed as a candidate retarder for MPC and showed a similar effect to boric acid<sup>22</sup>. Here, we proposed using this polymer in a cross-linked hydrogel form by a controlled calcium ionic release from calcium carbonate using  $\delta$ -gluconolactone at various ratios. As a result of preliminary experiments, different groups of modifications were proposed for MPC using variable concentrations of sodium alginate (SA: 1.25 or 1.5%), powder-to-liquid ratios (P/L: 2.0 or 2.5) and cross-linking system ratios (GDL/CC: 90/120 or 120/150). The use of the parameters mentioned earlier significantly impacted on the obtained characteristics of cements, particularly: application properties (setting time, reaction temperature, paste's cohesion and injectability), hydraulic reaction efficiency, porosity and wettability, degradation behavior,

cellular response and mechanical properties. The conducted research allowed for selecting the optimal obtaining method for MPC cement with improved properties dedicated to medical applications, potentially offering a more favorable alternative to the currently used CPC cements.

The hydration reaction of magnesium phosphate cement depends on various parameters, such as MgO particle size, magnesia reactivity, Mg-to-P ratio, powder-to-liquid ratio and mixing method<sup>5,11,30</sup>. The clinically accepted setting time should be between 10 and 20 min for optimal cement application<sup>32</sup>. Further, several studies showed that tissue exposure of more than 1 min to temperature over 50 °C causes bone tissue necrosis, hence the cement reaction temperature should be lower<sup>33,34</sup>. Unfortunately, the above-mentioned parameters have limited effectiveness and often, the MPC reaction has an inadequate setting time and occurs at high temperatures; therefore, various retarders are additionally used<sup>35</sup>. Another option proposed here is to create a composite cement by incorporating a polymer component. The addition of SA shortened the MPC cement's setting time in all cases, even without cross-linking. However, the differences between SA 1.25% and 1.50% are probably related to the number of tested specimens and the not precise measurement method. Further, depending on the parameters, it had a different effect on the reaction temperature—significantly increasing or slightly decreasing it (Table 2). The shortest setting times (below 10 min) at the highest temperatures (above 58 °C) were obtained for the 1.25% SA groups. Increasing the polymer content (up to 1.50%) resulted in a less significant decrease in setting time (~1.5–3 min) but with no adverse effect on temperature rise (below ~49 °C). It has been shown in the literature that polymer additives may act as an effective retarder of MPC setting reactions. For example, oxygen-carboxymethyl chitosan (up to 5 wt%), acrylic latex (up to 5 wt%), carboxymethyl chitosan-alginate (up to 4 wt%) contributed to the delay of MPC hydration reaction and lowering its maximum temperature<sup>12,14,36</sup>. An opposite effect was observed in our experiments, possibly related to the hydrogel cross-linking. This additional reaction may cause indirect changes in the cement P/L ratio—as the cross-linking may block access to the water for the hydration reaction, thus setting proceeds more intensively. On the other hand, adding a polymer component should lower the reaction temperature by acting as a specific insulator. However, it should be remembered that in the studies mentioned above, the concentration of the polymer additive was much higher than that applied in our study. Further, Zárýbická et al. also obtained different results in the case of cross-linked polyvinyl alcohol (5 wt%) additive—the reaction temperature of MPC increased, but its setting time extended from 9.5 min to even 34/35 min<sup>13</sup>. Here, we did not confirm this behavior, likely since the concentration of sodium alginate was only up to 1.50%.

The proposed modification did not negatively affect the cement setting reaction as in the microstructure of each group, the precipitated magnesium phosphate crystals were found (Fig. 1). However, each of the studied cements differed in both the size of the crystals and their potential to grow. Further, for two cement groups, the formation of flower-like structures was additionally observed, which may be related to the encapsulation of the emerging crystals in the hydrogel matrix. SA itself was not visible in the structure of cements—it did not form separate agglomerates but evenly covered the ceramic crystals. These results contradict those previously obtained for modified MPC, such as citric acid<sup>8</sup> or cross-linked polyvinyl alcohol<sup>13</sup>. In those works with higher polymer concentrations, the polymer phase was visible in the MPC microstructure as a film covering the crystals and filling the pores. The GDL additive used in our dual-setting cements contributed to lowering the pH of the mixture (Fig. S2), but it did not have a negative impact on the hydration reactions. The observed pH curves are similar to neat MPC and consist of three typical stages, which enable the dissolution of MgO, the formation of gel-like k-struvite and its crystallization. This was confirmed by our XRD studies (Fig. 2) as all cements had the crystallized structure without any distinct amorphous areas. The formed cements consisted mainly of well-crystallized k-struvite ( $\text{MgKPO}_4 \times 6 \text{H}_2\text{O}$ ) and unreacted magnesium oxide. The presence of MgO in XRD patterns is a typical phenomenon previously observed for pure ceramic cements<sup>37</sup>. The applied modifications may not have a significant impact on the percentage of k-struvite to magnesium oxide or, in some groups, may even have a positive effect (Table S3)—observed for the cements with crystals in the form of flowers. This observed phenomenon may be related to the change in paste pH caused by the use of gluconolactone, which accelerated the dissolution of MgO. Further, due to the low content of SA, the characteristic bands were not found in the XRD spectra. Based on XRD analysis, we do not find any secondary hydration products of MPC with sodium alginate. Similar observations for dual-setting MPC cement have already been reported in the literature<sup>13</sup>. Further, the differences in the intensity of diffractograms (mainly due to various MgO content) may result from the water replacement by sodium alginate solutions, which have different physical properties (e.g., viscosity) or also due to changes in the P-L ratio of cements. Also, similar conclusions were made for adding acrylic latexes to MPC<sup>12</sup>. Generally, reducing unreacted magnesium oxide content in MPC cement has a positive effect as excessive MgO residues increase the pH and reduce the material's biocompatibility<sup>38,39</sup>. ATR-IR analysis did not indicate any alterations in the MPC standard vibration mode for any of the applied modifications with SA. Further, any newly formed bonds were not found in MPC + SA spectra other than the additional peaks characteristic for cross-linked alginate hydrogel. We performed an analysis of the SA cross-linking process applied here (Fig. S3), which indicated that the  $\text{Ca}^{2+}$  ions cross-link hydroxyl and carboxylate groups of alginate to form a chelating structure<sup>40,41</sup>. As a result of these interactions, the absorption region of stretching vibration of hydroxyl bonds in the sodium alginate spectrum appeared wider than in the case of cross-linked alginate spectra<sup>42</sup>. This phenomenon happens due to the Ca substitution of Na in the alginate block that changes the charge density, the radius and the atomic weight of the cation<sup>43</sup>. We found the shifts of peaks attributed to the asymmetric stretching vibration of the carboxylate group in our modified cement (Fig. 3—marked with numbers), which confirmed the effective cross-linking of sodium alginate in the ceramic matrix. The asymmetric  $-\text{COO}-$  vibration peak shifts to a lower wavenumber after using  $\text{CaCO}_3$  with GDL, which confirms strong interaction with calcium ions<sup>44</sup>. However, due to the high MPC cement mass fraction, some SA peaks are covered by the MPC peaks (especially close to  $1000 \text{ cm}^{-1}$ ). We could not find results for comparison in the literature regarding dual-setting MPC cements with incorporated hydrogel phase. However, our observations of the chemical structure of composite MPC are similar to research

on incorporating polymer additives into ceramic matrix<sup>14,36</sup>. Further, there are reports that Mg ions can also cross-link SA, whereas, a concentration approximately 5–10 times higher than for calcium ions and a longer reaction time of approximately 2–3 h would be required<sup>45</sup>. Hence we do not assume this phenomenon to occur here.

The MPC modification resulted in most cases in a decrease in the initial porosity of the cement (Table 3). The groups that showed a reduction in crystal size in SEM analysis (Fig. 1) had much lower porosity (~3.5–5.0%), which could be caused by a large number of crystals and their closing of free spaces in the matrix. On the other hand, the addition of hydrogel also could block the pores before its biodegradation. However, the porosity values are different for groups that created flower-like structures. MPC + 1.25%SA\_2.0P/L\_120/150GDL/CC has a porosity similar to or slightly greater than that of pure cement (~7.7–9.9%), while 1.50%SA\_2.5P/L\_90/120GDL/CC has the lowest porosity of all groups (~2.6%). The reason for this may be differences in the hydration reaction and, as a result, obtaining a different internal structure for both groups.

A reduction in the porosity of composite MPC or dual-setting cements was also noted previously in various studies<sup>12–14</sup>. Using sodium alginate in MPC cement in most groups did not result in significant changes in wettability nature, and all cements were hydrophilic (contact angle: ~5.5–30.6°). The MPC + 1.50%SA\_2.5P/L\_90/120GDL/CC showed the highest contact angle (~22.1°) as the only significant change after modification. This may be directly related to the addition of SA, which has a contact angle of about 42°<sup>46</sup>, or the specific microstructure of this group (structure with crystals in the form of flowers – Fig. 1 and low porosity – Table 3).

Injectability is an essential property of modern biomaterials, enabling their application in minimally invasive procedures. Ceramic cements, such as MPC, have such a feature, but it is highly problematic and depends on various technological parameters<sup>47</sup>. The proposed cements based on MPC + SA had improved injectability, and we also found that the cohesion of cement paste in the PBS solution was significantly better compared to pure cement (Fig. 5). Inadequate cohesion of cement in an aqueous environment may contribute to its improper material hardening and lack of adequate mechanical support<sup>48</sup>. MPC cement itself was well injectable, but its cohesion was very poor. The cross-linked polymer modification increased the stability of the paste and its resistance to washing out by creating a compact hydrogel structure for hardening the paste. The most advantageous in the application aspect were two groups, which also showed flower-like structures in the SEM analysis (Fig. 1). Our results consisted of other studies on MPC with polymer-added cements<sup>36,49</sup>. However, it should be noted that the studies conducted here were preliminary and qualitative in nature. For a more detailed analysis and comparison with the literature, it would be recommended to use a standardized method to determine the force required for paste extrusion and the percentage of paste injected. Further, in the future, an evaluation of the paste's viscosity is also recommended<sup>50,51</sup>.

A significant advantage of magnesium phosphate cements over other ceramic cements, such as CPC, is their effective biodegradation. While CPCs may persist for several years, magnesium phosphate cements degrade more efficiently<sup>11</sup>. We have found that the SA hydrogel additive contributed to the acceleration of the cement degradation as increased weight losses (~1.5–4.0%) after a month of incubation were observed (Fig. 6). The differences in the results may be related to the different degradation rate of the SA hydrogel itself, caused by changes in porosity and microstructure of the specimens. However, it may also be caused by the different shares of unreacted magnesia in cements. For example, the most significant degradation was noted for MPC + 1.50%SA\_2.0P/L\_90/120GDL/CC, and the highest share of non-reacted MgO characterized this group, and testing may have caused it to wash out. Moreover, appropriate results were also observed for the MPC + 1.25%SA\_2.0P/L\_120/150GDL/CC (~3.0%) and 1.50%SA\_2.5P/L\_90/120GDL/CC (~2.0%), which showed flower-like structures in the microstructure, but significantly differed in porosity. Similar results to our finding were observed for MPC with the addition of oxygen-carboxymethyl chitosan<sup>14</sup>. On the other hand, the opposite conclusion was made by Yu et al., who observed no effect on MPC degradation after citric acid modification<sup>8</sup>. Hence, these differences may be related to the use of different polymers with various concentrations, but also may result from different research procedures (e.g. the amount of solvent or the frequency of its replacement).

The creation of a mineralized apatite layer on the material's surface significantly improves the connection between the implant and bone tissue, fostering better integration<sup>52</sup>. The assessment of a biomaterial's bioactivity usually involves conducting incubation within simulated body fluid environments<sup>53</sup>. However, MPC shows a low ability to mineralize apatite, which has been observed in the studies conducted so far<sup>54</sup>. Here, after PBS incubating for a month, the tested cement surfaces exhibited deposits, presumptively hydroxyapatite (Fig. 7), a phenomenon similarly noted by Zhou et al. in their study on MPC preparation using microwave technology<sup>55</sup>. This limitation is attributed to the action of Mg<sup>2+</sup> serving as an effective inhibitor of apatite mineral crystallization<sup>56</sup>. Concurrently, the degradation process experienced by the MPC cement matrix may complicate mineral deposition, as the deteriorating surface hampers proper adhesion.

Depending on its preparation, MPC cement can reach a compressive strength of 10–50 MPa, while human cortical bone has about 90–190 MPa<sup>57,58</sup>. Hence, for load-bearing applications, it is customarily accepted that this requirement should be met. Whereas the actual loads related to everyday functioning are much lower than the maximum—which was confirmed, for example, by L. Schroeter et al.<sup>59</sup> in an *in vivo* study with a bone cement treatment of a defect model of a merino sheep proximal tibia. They found that the cement with a compressive strength of 4–12 MPa was enough for the proper functioning of the animal during the typical load-bearing application and ensured healing of the bone defect. Further, some reports suggest that a small amount of unreacted MgO contributes to the increase in mechanical strength. However, an excess of unreacted MgO lead to the cement's structural instability and a reduction in its strength<sup>60</sup>. Here, the polymer additive did not contribute to the improvement of the mechanical characteristics of MPC cement and, unfortunately, in most groups, caused a decrease in compressive strength (Fig. 8). This may be partially related to the reduction in the share of MgO in the cement structure (Tab. S3). Moreover, there was no trend with increasing the SA concentration or internal porosity and worsening the mechanical strength. However, no negative impact was confirmed only for the MPC + 1.50%SA\_2.5P/L\_90/120GDL/CC cement, which was characterized by the lowest porosity (~2.6%), a

crystalline structure in the form of a flower, high percentage share of k-struvite (~78%), the highest wettability (~22.5%) and high cohesion. In the case of Young's modulus, all tested groups showed its lowering (from ~7.0 to ~3.0–5.5 GPa)-which may also mean a reduction in brittleness by obtaining a „pseudo-plastic effect“. Reports suggest that an additional polymer phase in the ceramic matrix is a barrier to crack propagation. For example, it was observed that the incorporation of carboxymethyl chitosan-alginate (up to 2%) into MPC or citric acid (up to 0.04 g/mL) into MPC modified with calcium dihydrogen phosphate results in doubling the compressive strength (CS: ~50 MPa)<sup>8,36</sup>. Also, modification with cross-linked polyvinyl alcohol contributed to the improvement of its mechanical strength (CS: ~35 MPa) and its Young Modulus (YM: ~850 MPa)<sup>13</sup>. On the other hand, in the research of Wang et al., it has been shown that the addition of citric acid and calcium carbonate (up to 5%) contributes to increasing the porosity of cement, which results in a significant reduction in mechanical properties (CS: ~12 MPa)<sup>49</sup>. Moreover, to validate the potential of SA to contribute as a barrier to crack progression, additional fracture toughness studies should be conducted in the future.

In general, it is assumed that modern biomaterials should actively support bone regeneration, and research on MPC confirms its high effectiveness in treating bone defects<sup>58</sup>. It has also been proven that released Mg ions have an anti-osteoporotic effect as they increase the proliferation of osteoblasts and, at the same time, inhibit osteoclast formation and their function<sup>61</sup>. Further, it was confirmed that magnesium phosphate cement is a fully biocompatible material and may be used in regenerative medicine<sup>62</sup>. Here, we conducted biological experiments to check whether the applied modification does not disturb the biological properties of cement and how it affects the cellular response. Notwithstanding, it should be remembered that due to the high bioactivity of the MPC ceramics and ion release into the cell culture medium or exchange for forming specific hydroxyapatite on the cement surface<sup>63</sup>, conducting *in vitro* studies is somewhere problematic. Hence, an additional pre-treatment was necessary and applied for tested specimens before experiments to equalize the magnesium and phosphate ions<sup>26</sup>. However, due to the increased biodegradation of modified groups, there was a risk of disturbance of the ionic balance. Therefore, the results may be inconsistent with the actual *in vivo conditions*, where body fluids continuously flow to remove ionic degradation products<sup>64</sup>. The above arguments may explain the negative trend associated with the decreasing osteoblast viability for the MPC + SA groups (Fig. 9). Whereas, aside from these problems, the conducted study confirmed that the three groups of cements are classified as cytocompatible (viability 70% compared to control – ISO 10993-5 standard<sup>65</sup> and no statistically significant change compared to MPC). There is no clear trend related to unreacted MgO, porosity, wettability or degradation and cellular response. Hence, the differences could be influenced by various microstructures of cements (Fig. 1), the potential for hydroxyapatite production or even by the different amounts of ions released into the culture medium. Moreover, this study indicated that the MPC + 1.25%SA\_2.0P/L\_120/150GDL/CC group is the least cytocompatible (~67.9% MTT) and is not recommended for medical applications. Composite cements have previously been tested for their cellular response. For example, MPC with oxygen-carboxymethyl chitosan and carboxymethyl chitosan-alginate showed no significant effect on the viability of MC3T3-E1 cells after 24 h compared to pure MPC<sup>14,36</sup>. And also, the addition of citric acid into MPC with calcium dihydrogen phosphate had a similar effect on mBMS cells<sup>8</sup>.

The research shows that MPC + 1.50%SA\_2.5P/L\_90/120GDL/CC bone cement may be recommended for medical applications. This material is characterized by appropriate injectability, and its paste is resistant to leaching. The cement set in ~12 min at a temperature below 50 °C, forming well-crystallized k-struvite (~78%) with cross-linked alginate hydrogel. It is hydrophilic (~22%), exhibits low initial porosity (~3%) and degrades effectively (~2%/month). It also demonstrates the potential for apatite formation on its surface. This material has a compressive strength similar to pure cement (~33 MPa) with reduced brittleness (Young Modulus: ~4.8 GPa). Further, cement, despite its high bioreactivity, remained cytocompatible (cell viability above 70% compared to TCP). Thus, this cement seems suitable as an injectable bone substitute with a high potential for effectively treating various bone defects or diseases. Additionally, this cement may serve as an alternative to CPC cements, as it is characterized by a much faster binding reaction, high rate of biodegradation, superior mechanical properties, and suitable injectability.

## Conclusion

In the present study, we successfully developed a novel dual-setting bone cement by combining magnesium potassium phosphate with cross-linked alginate hydrogel. This biocomposite cures in two reactions: an acid-base hydration reaction of magnesium phosphate and an ionic cross-linking reaction of sodium alginate. The incorporation of polymer into MPC cement significantly influenced its various properties but did not negatively affect its phase structure, and obtaining k-struvite crystals was confirmed. Various technological parameters for producing such cements were tested, and the optimal modified groups were selected. The cements showed a shortened setting reaction, diverse microstructure, increased wettability and degradability and improved paste cohesion and injectability. Despite increased bioreactivity, most of the tested groups remained cytocompatible. The reduced Young's Modulus may indicate a „pseudo-plastic effect“ for ceramic-polymer cements, while the compressive strength after modification showed an unfavorable trend. Bone cement based on MPC with 1.50% SA using a powder-to-liquid ratio of 2.5 g/mL and cross-linking ratio 90/120 of GDL/CC seems to be a favorable candidate for potential clinical application for minimally invasive procedures.

## Data availability

The datasets generated during and analysed during the current study are available from the corresponding author on reasonable request.

## References

- Wang, P. & Wang, X. Mimicking the native bone regenerative microenvironment for in situ repair of large physiological and pathological bone defects. *Eng. Regen.* **3**, 440–452 (2022).
- Wei, M. *et al.* Enhanced mechanical properties and anti-washout of calcium phosphate cement/montmorillonite composite bone-cement for bone-repair applications. *Ceram. Int.* **48**, 35185–35197 (2022).
- Albrektsson, T., & Johansson, C. Osteoinduction, osteoconduction and osseointegration. *Eur. Spine J.* **10**, 96–S101 (2001).
- Goldberg, M. A. *et al.* Magnesium-substituted calcium phosphate cements with  $(Ca + Mg)/P = 2$ . *Chem. Technol.* **467**, 100–104 (2016).
- Le Rouzic, M., Chaussadent, T., Stefan, L. & Saillio, M. On the influence of Mg/P ratio on the properties and durability of magnesium potassium phosphate cement pastes. *Cem. Concr Res.* **96**, 27–41 (2017).
- Tan, Y. *et al.* Optimization of magnesium potassium phosphate cements using ultrafine fly ash and fly ash. *ACS Sustain. Chem. Eng.* **11**, 3194–3207 (2023).
- Walling, S. A., & Provis, J. L. Magnesia-based cements: A journey of 150 years, and cements for the future. *Chem. Rev.* **116**, 4170–4204 (2016).
- Yu, S., Liu, L., Xu, C. & Dai, H. Magnesium phosphate based cement with improved setting, strength and cytocompatibility properties by adding  $Ca(H_2PO_4)_2 \cdot H_2O$  and citric acid. *J. Mech. Behav. Biomed. Mater.* **91**, 229–236 (2019).
- Ma, H., Xu, B., Liu, J., Pei, H. & Li, Z. Effects of water content, magnesia-to-phosphate molar ratio and age on pore structure, strength and permeability of magnesium potassium phosphate cement paste. *Mater. Des.* **64**, 497–502 (2014).
- Yuan, Z. *et al.* Controlled magnesium ion delivery system for in situ bone tissue engineering. *J. Control Release.* **350**, 360–376 (2022).
- Yu, Y., Xu, C. & Dai, H. Preparation and characterization of a degradable magnesium phosphate bone cement. *Regen. Biomater.* **3**, 231–237 (2016).
- Zárybnická, L., Machotová, J., Mácová, P., Machová, D. & Viani, A. Design of polymeric binders to improve the properties of magnesium phosphate cement. *Constr. Build. Mater.* **290**, 123202 (2021).
- Zárybnická, L., Mácová, P. & Viani, A. Properties enhancement of magnesium phosphate cement by cross-linked polyvinyl alcohol. *Ceram. Int.* **48**, 1947–1955 (2022).
- Gong, C. *et al.* Enhancing the mechanical properties and cytocompatibility of magnesium potassium phosphate cement by incorporating oxygen-carboxymethyl Chitosan. *Regen. Biomater.* **8**, 1–10 (2021).
- Tang, Z. *et al.* Impact of polyethylene fiber on the ductility and durability of magnesium phosphate cement. *J. Build. Eng.* **68**, 106123 (2023).
- Tan, J. *et al.* Development of alginate-based hydrogels: Crosslinking strategies and biomedical applications. *Int. J. Biol. Macromol.* **239**, 124275 (2023).
- Ahmad Raus, R., Wan Nawawi, W. M. F. & Nasaruddin, R. R. Alginate and alginate composites for biomedical applications. *Asian J. Pharm. Sci.* **16**, 280–306 (2021).
- Cao, H., Duan, L., Zhang, Y., Cao, J. & Zhang, K. Current hydrogel advances in physicochemical and biological response-driven biomedical application. *Div. Signal. Trans. Target. Ther.* **6**, 426 (2021).
- Gombotz, W. R. & Wee, S. F. Protein release from alginate matrices. *Adv. Drug Deliv Rev.* **64**, 194–205 (2012).
- Varaprasad, K., Jayaramudu, T., Kanikireddy, V., Toro, C. & Sadiku, E. R. Alginate-based composite materials for wound dressing application: A mini review. *Carbohydr. Polym.* **236**, 116025 (2020).
- Wei, Q. *et al.* Modification, 3D printing process and application of sodium alginate based hydrogels in soft tissue engineering: A review. *Int. J. Biol. Macromol.* **232**, 123450 (2023).
- Liu, R., Fang, B., Zhang, G., Guo, J. & Yang, Y. Investigation of sodium alginate as a candidate retarder of magnesium phosphate cement: Hydration properties and its retarding mechanism. *Ceram. Int.* **48**, 30846–30852 (2022).
- Su, C., Li, D., Wang, L. & Wang, Y. Green Green double crosslinked starch-alginate hydrogel regulated by sustained calcium ion-gluconolactone release for human motion monitoring. *Chem. Eng. J.* **455**, 140653 (2023).
- Lakrat, M., Mejdoubi, E. M., Ozdemir, F. & Santos, C. Effect of sodium silicate concentration on the physico-chemical properties of dual-setting bone-like apatite cements. *Mater. Today Commun.* **31**, 103421 (2022).
- Growney Kalaf, E. A., Pendyala, M., Bledsoe, J. G. & Sell, S. A. Characterization and restoration of degenerated IVD function with an injectable, in situ gelling alginate hydrogel: An in vitro and ex vivo study. *J. Mech. Behav. Biomed. Mater.* **72**, 229–240 (2017).
- Przekora, A. The summary of the most important cell-biomaterial interactions that need to be considered during in vitro biocompatibility testing of bone scaffolds for tissue engineering applications. *Mater. Sci. Eng. C.* **97**, 1036–1051 (2019).
- Sena, H. J., da Silva, F. V. & Fileti, A. M. F. ANN model adaptation algorithm based on extended kalman filter applied to pH control using MPC. *J. Process. Control.* **102**, 15–23 (2021).
- Yan, B. *et al.* Research and development of a sodium alginate/calcium ion gel based on in situ cross-linked double-network for controlling spontaneous combustion of coal. *Fuel.* **322**, 124260 (2022).
- Almulaiky, Y. Q. & Al-Harbi, S. A. Preparation of a calcium alginate-coated polypyrrole/silver nanocomposite for site-specific immobilization of polygalacturonase with high reusability and enhanced stability. *Catal. Lett.* **152**, 28–42 (2022).
- Xu, B., Winnefeld, F., Kaufmann, J. & Lothenbach, B. Influence of magnesium-to-phosphate ratio and water-to-cement ratio on hydration and properties of magnesium potassium phosphate cements. *Cem. Concr Res.* **123**, 105781 (2019).
- Gelli, R., Mati, L., Ridi, F. & Baglioni, P. Tuning the properties of magnesium phosphate-based bone cements: Effect of powder to liquid ratio and aqueous solution concentration. *Mater. Sci. Eng. C.* **95**, 248–255 (2019).
- Jia, J. *et al.* Development of magnesium calcium phosphate biocement for bone regeneration. *J. R Soc. Int.* **7**, 1171–1180 (2010).
- Shi, Y. *et al.* Bioactive magnesium phosphate cement incorporating chondroitin sulfate for bone regeneration. *Biomed. Mater.* **16**, 035034 (2021).
- Li, C. *et al.* Injectable and bioactive bone cement with moderate setting time and temperature using borosilicate bio-glass-incorporated magnesium phosphate. *Biomed. Mater.* **15**, 045015 (2020).
- Yao, Y. W. *et al.* Research progress on the effects of retarders on the properties and hydration mechanism of magnesium phosphate cement. *J. Mater.* **36**, 1–7 (2022).
- Yu, L. *et al.* Carboxymethyl Chitosan-Alginate enhances bone repair effects of magnesium phosphate bone cement by activating the FAK-Wnt pathway. *Bioact Mater.* **20**, 598–609 (2023).
- Ribeiro, D. V., Paula, G. R. & Morelli, M. R. Use of microwave oven in the calcination of MgO and effect on the properties of magnesium phosphate cement. *Constr. Build. Mater.* **198**, 619–628 (2019).
- Li, Y., Sun, J. & Chen, B. Experimental study of magnesia and M/P ratio influencing properties of magnesium phosphate cement. *Constr. Build. Mater.* **65**, 177–183 (2014).
- Yu, Y. *et al.* Evaluation of inherent toxicology and biocompatibility of magnesium phosphate bone cement. *Col Surf. B Biointer.* **76**, 496–504 (2010).
- Voo, W. P. *et al.* Production of ultra-high concentration calcium alginate beads with prolonged dissolution profile. *RSC Adv.* **5**, 36687–36695 (2015).

41. Maxwell, C. J. *et al.* Tunable Alginate hydrogels as injectable drug delivery vehicles for optic neuropathy. *J. Biomed. Mater. Res. A* **110**, 1621–1635 (2022).
42. Nastaj, J., Przewłocka, A. & Rajkowska-Myśliwiec, M. Biosorption of Ni(II), pb(II) and zn(II) on calcium alginate beads: Equilibrium, kinetic and mechanism studies. *Pol. J. Chem. Tech.* **18**, 81–87 (2016).
43. Li, J., He, J., Huang, Y., Li, D. & Chen, X. Improving surface and mechanical properties of alginate films by using ethanol as a co-solvent during external gelation. *Carbohydr. Polym.* **123**, 208–216 (2015).
44. Li, J., Wu, Y., He, J. & Huang, Y. A new insight to the effect of calcium concentration on gelation process and physical properties of alginate films. *J. Mater. Sci.* **51**, 5791–5801 (2016).
45. Topuz, F., Henke, A., Richtering, W. & Groll, J. Magnesium ions and alginate do form hydrogels: A theological study. *Soft Matter* **8**, 4877 (2012).
46. Pereira, R. F., Carvalho, A., Gil, M. H., Mendes, A. & Bártolo, P. J. Influence of aloe vera on water absorption and enzymatic in vitro degradation of alginate hydrogel films. *Carbohydr. Polym.* **98**, 311–320 (2013).
47. O'Neill, R. *et al.* Critical review: Injectability of calcium phosphate pastes and cements. *Acta Biomater.* **50**, 1–19 (2017).
48. Alkhraisat, M. H. *et al.* The effect of hyaluronic acid on brushite cement cohesion. *Acta Biomater.* **5**, 3150–3156 (2009).
49. Wang, J. *et al.* An injectable porous bioactive magnesium phosphate bone cement foamed with calcium carbonate and citric acid for periodontal bone regeneration. *J. Mech. Behav. Biomed. Mater.* **142**, 105805 (2023).
50. Weichhold, J., Goetz-Neunhoeffler, F., Hurler, K. & Gbureck, U. Pyrophosphate ions inhibit calcium phosphate cement reaction and enable storage of premixed pastes with a controlled activation by orthophosphate addition. *Ceram. Int.* **48** (11), 15390–15404 (2022).
51. Cassel, J. B., Tronco, M. C., Paim, T. C., Wink, M. R. & dos Santos L. A. L. Reinforcement of injectable premixed  $\alpha$ -tricalcium phosphate cements with silk fibroin solutions. *Mater. Today Commun.* **38**, 108440 (2024).
52. Liu, W., Zhai, D., Huan, Z., Wu, C. & Chang, J. Novel tricalcium silicate/magnesium phosphate composite bone cement having high compressive strength, in vitro bioactivity and cytocompatibility. *Acta Biomater.* **21**, 217–227 (2015).
53. Kokubo, T. & Takadama, H. How useful is SBF in predicting in vivo bone bioactivity? *Biomaterials* **27**, 2907–2915 (2006).
54. Liu, W., Huan, Z., Wu, C., Zhou, Z. & Chang, J. High-strength calcium silicate-incorporated magnesium phosphate bone cement with osteogenic potential for orthopedic application. *Compos. B Eng.* **247**, 110324 (2022).
55. Zhou, H., Agarwal, A. K., Goel, V. K. & Bhaduri, S. B. Microwave assisted preparation of magnesium phosphate cement (MPC) for orthopedic applications: A novel solution to the exothermicity problem. *Mater. Sci. Eng. C* **33** (7), 4288–4294 (2013).
56. Staiger, M. P., Pietak, A. M., Huadmai, J. & Dias, G. Magnesium and its alloys as orthopedic biomaterials: A review. *Biomaterials* **27** (9), 1728–1734 (2006).
57. Henkel, J. *et al.* Bone regeneration based on tissue engineering conceptions—a 21st century perspective. *B Res.* **1**, 216–248 (2013).
58. Ostrowski, N., Roy, A. & Kumta, P. N. Magnesium phosphate cement systems for hard tissue applications: A review. *ACS Biomater. Sci. Eng.* **2**, 1067–1083 (2016).
59. Schröter, L. *et al.* Ready-to-use and rapidly biodegradable magnesium phosphate bone cement: In vivo evaluation in Sheep. *Adv. Healthc. Mater.* **12**, 1–15 (2023).
60. Haque, M. A. & Chen, B. In vitro and in vivo research advancements on the magnesium phosphate cement biomaterials: A review. *Materia (Oxf)* **13**, 100852 (2020).
61. Janning, C. *et al.* Magnesium hydroxide temporarily enhancing osteoblast activity and decreasing the osteoclast number in peri-implant bone remodelling. *Acta Biomater.* **6**, 1861–1868 (2010).
62. Fang, B. *et al.* Research progress on the properties and applications of magnesium phosphate cement. *Ceram. Int.* **49**, 4001–4016 (2023).
63. Großardt, C., Ewald, A., Grover, L. M., Barralet, J. E. & Gbureck, U. Passive and active in vitro resorption of calcium and magnesium phosphate cements by osteoclastic cells. *T Eng. Part. A* **16**, 3687–3695 (2010).
64. Kaiser, F. *et al.* Accelerated bone regeneration through rational design of magnesium phosphate cements. *Acta Biomater.* **145**, 358–371 (2022).
65. ISO 10993. 5:2009 standard: Biological Evaluation of Medical Devices.

## Acknowledgements

The authors thank all those who contributed to preparing this paper. i.e., the team from the Biomaterials and the Ceramics Groups at the Gdańsk University of Technology (especially D. Jaworski and Joanna Sypniewska), and the team from the Medicinal Chemistry Research Group at Nicolaus Copernicus University in Toruń (especially D. Chełminiak-Dudkiewicz, PhD) for their support in the fabrication of cement powder and/or technical assistance in some of the tests.

## Author contributions

Conceptualization. M.W. and J.K.; methodology. M.W., J.K., D.K., A.R. and U.G.; formal analysis. M.W., R.J., D.K., J.K. and U.G.; investigation. R.J., A.M.-G., A.R., D.K., J.K. and M.W.; resources. M.W.; data curation. R.J., J.K., D.K. and M.W.; writing - original draft preparation. M.W.; writing - review and editing. M.W., J.K. and U.G.; visualization. M.W., A.M.-G. and J.K.; project administration. M.W.; supervision. M.W. and U.G. All authors have read and agreed to the published version of the manuscript.

## Funding

This research was supported by the Gdańsk University of Technology by the DEC-3/2022/IDUB/III.4.3/Pu grant under the PLUTONIUM 'Excellence Initiative – Research University' program.

## Competing interests

The authors declare no competing interests.

## Additional information

**Supplementary Information** The online version contains supplementary material available at <https://doi.org/10.1038/s41598-024-70984-5>.

**Correspondence** and requests for materials should be addressed to M.W.

**Reprints and permissions information** is available at [www.nature.com/reprints](http://www.nature.com/reprints).

**Publisher's note** Springer Nature remains neutral with regard to jurisdictional claims in published maps and institutional affiliations.

**Open Access** This article is licensed under a Creative Commons Attribution-NonCommercial-NoDerivatives 4.0 International License, which permits any non-commercial use, sharing, distribution and reproduction in any medium or format, as long as you give appropriate credit to the original author(s) and the source, provide a link to the Creative Commons licence, and indicate if you modified the licensed material. You do not have permission under this licence to share adapted material derived from this article or parts of it. The images or other third party material in this article are included in the article's Creative Commons licence, unless indicated otherwise in a credit line to the material. If material is not included in the article's Creative Commons licence and your intended use is not permitted by statutory regulation or exceeds the permitted use, you will need to obtain permission directly from the copyright holder. To view a copy of this licence, visit <http://creativecommons.org/licenses/by-nc-nd/4.0/>.

© The Author(s) 2024